

Differences in the Central Nervous System Distribution and Pharmacology of the Mouse 5-Hydroxytryptamine-6 Receptor Compared with Rat and Human Receptors Investigated by Radioligand Binding, Site-Directed Mutagenesis, and Molecular Modeling

WARREN D. HIRST, BJARKE ABRAHAMSEN, FRANK E. BLANEY, ANDREW R. CALVER, LUCIA ALOJ, GARY W. PRICE, and ANDREW D. MEDHURST

Neurology and GI Centre of Excellence for Drug Discovery (W.D.H., B.A., A.R.C., L.A., A.D.M.), Computational, Analytical and Structural Sciences (F.E.B.), and Psychiatry Centre of Excellence for Drug Discovery (G.W.P.), GlaxoSmithKline, Harlow, Essex, United Kingdom

Received June 26, 2003; accepted August 25, 2003

This article is available online at <http://molpharm.aspetjournals.org>

ABSTRACT

There is increasing evidence for a role of 5-hydroxytryptamine-6 (5-HT₆) receptors in cognitive function. In the rat and human brain, 5-HT₆ receptors are widely expressed and highly enriched in the basal ganglia. However, in the mouse brain, only very low levels of 5-HT₆ receptor mRNA and receptor protein, measured by TaqMan reverse transcriptase-polymerase chain reaction and selective radioligand binding, could be detected, with no evidence of enrichment in the basal ganglia. The mouse receptor was cloned and transiently expressed in human embryonic kidney 293 cells to characterize its pharmacological profile. Despite significant sequence homology between human, rat, and mouse 5-HT₆ receptors, the pharmacological profile of the mouse receptor was significantly different from the rat and human receptors. Four amino acid residues, con-

served in rat and human and divergent in mouse receptors, were identified, and various mutant receptors were generated and their pharmacologies studied. Residues 188 (tyrosine in mouse, phenylalanine in rat and human) in transmembrane region 5 and 290 (serine in mouse, asparagine in rat and human) in transmembrane region 6 were identified as key amino acids responsible for the different pharmacological profiles. Molecular modeling of the receptor and docking of selective and nonselective compounds was undertaken to elucidate the ligand receptor interactions. The binding pocket was predicted to be different in the mouse compared with rat and human 5-HT₆ receptors, and the models were in excellent agreement with the observed mutation results and have been used extensively in the design of further selective 5-HT₆ antagonists.

The 5-hydroxytryptamine-6 (5-HT₆) receptor is one of 14 distinct mammalian 5-HT (serotonin) receptors expressed in the central nervous system through which 5-HT exerts a wide variety of physiological and behavioral effects. The rat, human, and, more recently, mouse 5-HT₆ receptors have been cloned and are positively coupled to adenylyl cyclase when expressed in cell lines (Monsma et al., 1993; Ruat et al.,

1993; Kohen et al., 1996, 2001). The 5-HT₆ receptor has a unique pharmacological profile, including a high affinity for both typical, such as chlorpromazine and amoxapine, and atypical, such as clozapine and olanzapine, antipsychotics (Monsma et al., 1993; Roth et al., 1994; Kohen et al., 1996). Radiolabeled analogs of 5-HT₆ receptor antagonists have now been developed and characterized; both [³H]Ro 63-0563 and [¹²⁵I]SB-258585 have been shown to selectively label native 5-HT₆ receptors (Boess et al., 1998; Hirst et al., 2000). These tools have allowed the pharmacology of the 5-HT₆ receptors

This work was supported by GlaxoSmithKline.
W.D.H., B.A., and F.E.B. contributed equally to this work.

ABBREVIATIONS: 5-HT, 5-hydroxytryptamine; RT-PCR, reverse transcriptase-polymerase chain reaction; ECL2, second extracellular loop; HEK, human embryonic kidney; [³H]LSD, [*N*-methyl-³H]lysergic acid diethylamide; LSD, lysergic acid diethylamide; TM, transmembrane; GAPDH, glyceraldehyde-3-phosphate dehydrogenase; 5-MeO-T, 5-methoxytryptamine; SB-271046, 5-chloro-3-methyl-benzo[*b*]thiophene-2-sulfonic acid (4-methoxy-3-piperazin-1-yl-phenyl)-amide; SB-258510, 5-chloro-*N*-[4-methoxy-3-(4-methylpiperazin-1-yl)phenyl]-3-methyl-2-benzothiophene-sulfonamide; SB-258585, 4-iodo-*N*-[4-methoxy-3-(4-methylpiperazin-1-yl)-phenyl]-benzenesulfonamide; SB-214111, 4-bromo-*N*-[4-methoxy-3-(4-methylpiperazin-1-yl)-phenyl]-benzenesulfonamide; SB-357134, *N*-(2,5-dibromo-3-fluorophenyl)-4-methoxy-3-piperazin-1-ylbenzenesulfonamide; BRL-34849, *trans*-4a,5,6,7,12,12c-hexahydro-5-methyl-4H-5,7a-diazabenz[5,6]cyclohepta[1,2,3,4-*def*]fluorine; BRL-34969, *trans*-1,2,3,3a,4,5,9,14a-octahydro-3-methyldibenzo[*bef*]-pyrazino[3,2,1-*jk*][1]benzazepine; Ro 04-6790, 4-amino-*N*-(2,6 bis-methylamino-pyrimidin-4-yl)-benzene sulfonamide.

in the striatum to be fully characterized and compared with the recombinant receptors expressed in cell lines (Boess et al., 1998; Hirst et al., 2000).

In the rat brain, 5-HT₆ receptor mRNA, detected by Northern blot analysis, in situ hybridization, or RT-PCR, has been localized to the olfactory tubercle, nucleus accumbens, striatum, hippocampus, and cerebral cortex (Monsma et al., 1993; Ruat et al., 1993; Ward et al., 1995; Gerard et al., 1997; Grimaldi et al., 1998). Immunocytochemistry at the light and electron microscope levels have shown 5-HT₆ receptor-like immunoreactivity to be associated with dendritic processes in both the striatum and hippocampus of adult rats (Gerard et al., 1997; Hamon et al., 1998). These data are largely supported by a recent autoradiographic study with the use of the selective radioligand [¹²⁵I]SB-258585 (Roberts et al., 2002).

The distribution of the 5-HT₆ receptor in human brain is less well characterized. Northern blot analysis revealed highest expression levels of 5-HT₆ receptor mRNA in the caudate nucleus (Kohen et al., 1996), whereas a more recent study using receptor autoradiography investigated the distribution of 5-HT₆ receptors in postmortem samples from schizophrenic and normal patients and showed a distribution pattern similar to that in the rat brain (East et al., 2002).

The physiological role of 5-HT₆ receptors in the brain is not yet clearly understood. However, localization of 5-HT₆ receptors to both basal ganglia and limbic structures suggests that this receptor may participate in the serotonergic control of motor function, mood-dependent behavior, depression, and cognition. Before the development of selective 5-HT₆ receptor antagonists, studies using antisense oligonucleotides to reduce the number of receptors suggested that the 5-HT₆ receptor may be involved in the modulation of cholinergic neuronal function (Bourson et al., 1995), in increased 5-HT release induced by conditioned fear stress (Yoshioka et al., 1998) and in anxiogenic behavior (Hamon et al., 1998). Reports on the selective 5-HT₆ receptor antagonist Ro 04-6790 (Sleight et al., 1998; Bentley et al., 1999) suggest that this antagonist elicits behavioral effects similar to those described by the same group when they administered antisense oligonucleotides to the 5-HT₆ receptor (Bourson et al., 1995). In addition, studies with the selective 5-HT₆ receptor antagonists SB-271046, SB-357134, and Ro 04-6790 (Sleight et al., 1998; Bromidge et al., 1999, 2001; Routledge et al., 2000; Stean et al., 2002) support a role for 5-HT₆ receptors in cognitive function (Meneses, 2001; Rogers and Hagan, 2001; Woolley et al., 2001).

The present study was initiated after preliminary experiments in mouse brain homogenates suggested that there was no specific binding of the selective radioligand [¹²⁵I]SB-258585 to 5-HT₆ receptors. We therefore compared the distribution of 5-HT₆ receptor protein and mRNA in discrete regions of mouse, rat, and human brain. In addition, we cloned the mouse receptor and demonstrated that its pharmacological profile was markedly different from that of the other species. Site-directed mutagenesis studies were then performed to identify which of the few amino acid residues that differed between the species could be responsible for this pharmacological divergence. In addition, radioligand binding data on the wild-type and mutant receptors were used to explore the three-dimensional structure of the 5-HT₆ receptor. A preliminary account of some of the data have been presented in abstract form (Hirst et al., 2002).

Materials and Methods

Materials. [*N*-methyl-³H]lysergic acid diethylamide (³H]LSD) was purchased from Amersham Biosciences UK, Ltd. (Little Chalfont, Buckinghamshire, UK). [¹²⁵I]SB-258585 was synthesized, under contract, by Amersham Biosciences as described previously (Hirst et al., 2000). Lysergic acid diethylamide (LSD), 5-HT, mianserin, and methiothepin were from Sigma Chemical (Poole, Dorset, UK). SB-271046, SB-258510, SB-258585, SB-214111, SB-357134, BRL-34849, BRL-34969, and Ro 04-6790 were synthesized by Glaxo-SmithKline (Harlow, Essex, UK). The structures of these compounds are shown in Fig. 1. Cell culture reagents were obtained from Invitrogen (Paisley, UK). All other reagents were obtained from Sigma or Merck-BD (Lutterworth, Leicestershire, UK) and were of analytical grade.

Membrane Preparation and Radioligand Binding. Striatal tissue from adult male rats (Sprague-Dawley, 200–250 g; Charles River, Margate, Kent, UK), adult male mice [CD-1, 20 g (Charles River), and C57/BL6, 25 g (Harlan UK Ltd., Blackthorn, Bicester, UK)], and human caudate putamen tissue (from three nonidentifiable patients aged 64 to 76 years, whose cause of death was non-neurological, from Resource, Institute of Neurology, London, UK; approved by a local ethics committee) were prepared as described previously (Hirst et al., 2000).

Membranes were resuspended in a buffer containing 50 mM Tris-HCl, 10 μM pargyline, 5 mM MgCl₂, 5 mM ascorbate, and 0.5 mM EDTA, pH 7.4, and incubated with 0.1 nM [¹²⁵I]SB-258585 (specific activity, 2000 Ci/mmol) for 45 min at 37°C. Nonspecific binding was measured in the presence of 10 μM methiothepin. The experiments were terminated by rapid filtration through Whatman GF/B filters (Semat International, St. Albans, UK), pretreated with 0.3% (v/v) polyethylenimine, and washed with 9 ml of ice-cold buffer. Radioactivity was determined by gamma spectrometry using a Packard Cobra II gamma counter (PerkinElmer Life Sciences, Boston, MA). Protein concentrations were determined using the Bradford assay method (Bio-Rad protein assay kit; Bio-Rad, Hemel Hempstead, UK) using bovine serum albumin as a standard.

Distribution of 5-HT₆ Receptor mRNA Using TaqMan RT-PCR. TaqMan RT-PCR was carried out as described previously (Medhurst et al., 1999, 2000). Human poly(A⁺) mRNA samples were obtained from BD Biosciences Clontech (Palo Alto, CA), and rat and mouse total RNA was prepared in house using TRIzol reagent (Invitrogen). Oligo(dT)-primed cDNA synthesis was performed in triplicate using 200 ng of human poly(A⁺) mRNA or 1 μg of rat or mouse total RNA and Superscript II reverse transcriptase according to the manufacturer's instructions (Invitrogen). TaqMan PCR assays were performed in 96-well optical plates on an ABI Prism 7700 Sequence Detection system (Applied Biosystems, Foster City, CA) according to manufacturer's instructions. Primer sequences are shown in Table 1. Data were analyzed using the relative standard curve method, with each sample being normalized to GAPDH to correct for differences in RNA quality and quantity, and data were expressed as arbitrary units on a scale from 0 to 1 (Medhurst et al., 1999, 2000).

Cloning of 5-HT₆ Receptors. Human, rat, and mouse 5-HT₆ receptor cDNAs were cloned by nested PCR from marathon-ready cDNA obtained from whole brain (BD Biosciences Clontech). The PCR enzyme used was Platinum Taq DNA polymerase (Invitrogen). PCR was carried out according to the manufacturer's instructions (95°C for 2 min, then 30 cycles of 95°C for 30 s, 58°C for 30 s, and 72°C for 150 s, and then a final extension at 72°C for 7 min). Full-length bands were visualized by gel electrophoresis, TOPO-cloned into the mammalian expression vector pcDNA3.1/V5-His-TOPO (Invitrogen) according to manufacturer's instructions, and confirmed by DNA sequencing.

Site-Directed Mutagenesis. Primers, shown in Table 1, were designed to introduce each of the desired mutations. Mutagenesis experiments were performed with the QuikChange site-directed mu-

tagenesis kit (Stratagene, La Jolla, CA) with use of either wild-type mouse or rat 5-HT₆ receptor cDNA, in pcDNA 3.1, as a template.

All of the single mutations and the S175P/Y188F and S277G/S290N double mutations were made using the primers shown. The other mutations—Y188F/S277G, Y188F/S290N, Y188F/S277G/S290N, and S175P/Y188F/S277G/S290N—were generated by excising the insert in the S175P, Y188F, or the S175P/Y188F constructs using SfiI and HindIII and inserting into the appropriate vectors containing the S277G, S290N, or S277G/S290N mutations. All mutations were confirmed by DNA sequencing.

Cell Culture, Transfection, and Expression. Human embryonic kidney (HEK) 293 cells were maintained in Dulbecco's modified Eagle's medium supplemented with 10% dialyzed fetal calf serum and 1% nonessential amino acids. Exponentially growing cells were transfected using LipofectAMINE 2000 (Invitrogen) according to the manufacturer's instructions and then incubated for 48 h. The cells were harvested in phosphate-buffered saline, pelleted by centrifugation (1000g) and stored at -80°C before membrane preparation as described previously (Hirst et al., 2000).

Radioligand Binding to Transfected Cell Membranes. Binding assays were carried out in a buffer containing 50 mM Tris-HCl, 10 μ M pargyline, 5 mM MgCl₂, 5 mM ascorbate, and 0.5 mM EDTA, pH 7.4, and consisted of 50 μ l of displacing compound or buffer, 400 μ l of membrane suspension (corresponding to approximately 10–15 μ g protein/well), and 50 μ l of [³H]LSD (specific activity, 76–78 Ci/mmol). Nonspecific binding was measured in the presence of 10 μ M methiothepin. In competition binding experiments, 10 concentrations of the competing ligands were tested (concentration ranges,

0.03 nM to 1 μ M and 0.3 nM to 10 μ M) at a final [³H]LSD concentration of 2 nM. Equilibrium was attained by incubation at 37°C for 45 min, and the experiments were terminated by rapid filtration through Whatman GF/B 96-well filter plates (PerkinElmer Life Sciences) and washed with 5 ml of ice-cold buffer. Radioactivity was determined by liquid-scintillation spectrometry with the use of Top-Count NXT (PerkinElmer Life Sciences).

The concentration of drug inhibiting-specific radioligand binding by 50% (IC₅₀) was determined by iterative curve fitting (Bowen and Jerman, 1995). pK_i values for receptor binding were then calculated from the IC₅₀ values, as described by Cheng and Prusoff (1973), using the K_D values determined in previous saturation binding studies. Data are expressed as the mean \pm S.E. mean of at least three separate experiments. Statistical analysis of the binding affinities was performed using Student's *t* test (Statistica for Windows; StatSoft, Tulsa, OK).

Sequence Alignments and Transmembrane Region Predictions. The sequence alignment of the rat, mouse, and human receptors was performed using the Clustal W program (Thompson et al., 1994). Transmembrane (TM) regions were identified using the hydrophobic analysis algorithm described by Kyte and Doolittle (1982), as implemented in the "in-house" program GPCR_Builder (Blaney and Tennant, 1996), together with the information on the transmembrane regions of the rhodopsin structure.

5-HT₆ Receptor Modeling and Ligand Docking. The initial models of the TM regions of the rodent and human 5-HT₆ receptors were constructed by homology with the published X-ray crystal structure of bovine rhodopsin (Polczewski et al., 2000). Alignments

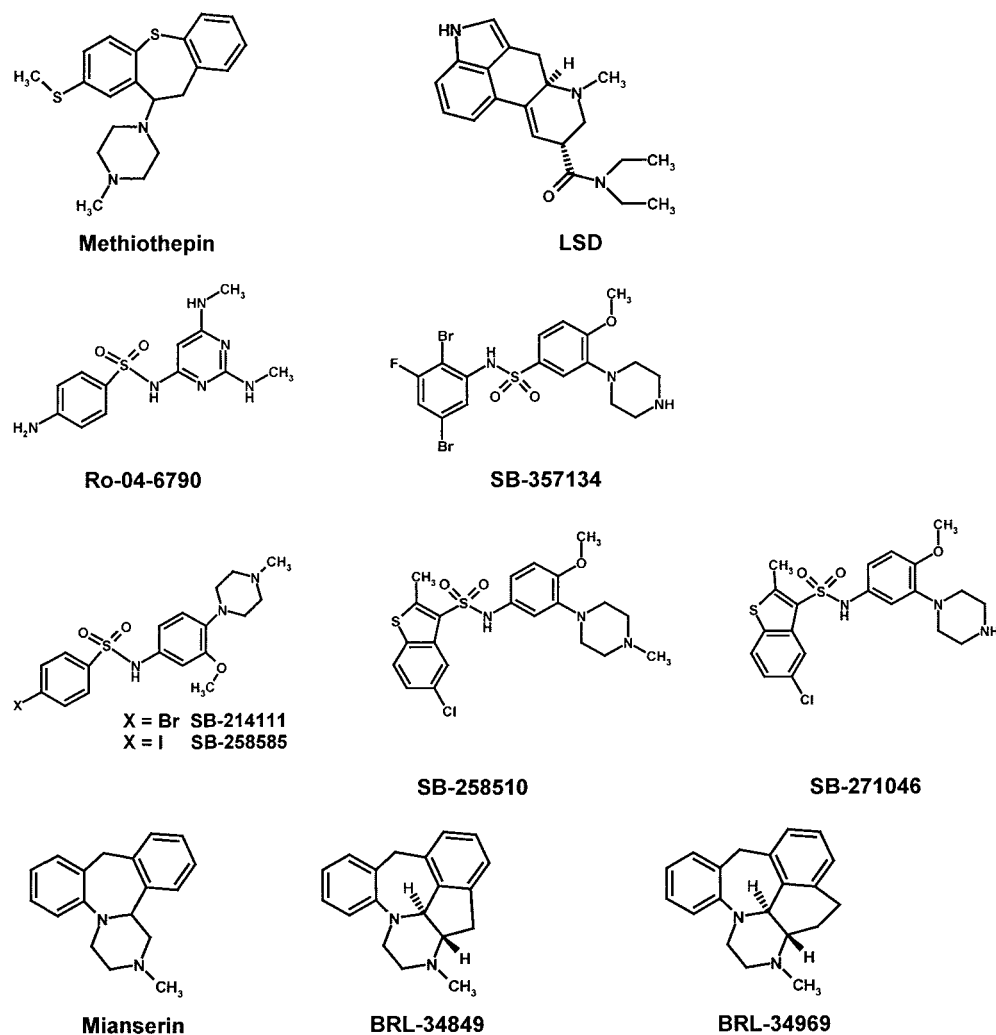


Fig. 1. Chemical structures of methiothepin, LSD, SB-271046, SB-258510, SB-258585, SB-214111, SB-357134, Ro 04-6790, BRL-34849, and BRL-34969.

between the 5-HT₆ sequences and bovine rhodopsin were derived from the classic motifs found in each TM region, namely the asparagine in TM1, the aspartate in TM2, the "DRY" motif (ERY in rhodopsin) of TM3, the tryptophan in TM4, and the conserved prolines in TM5, TM6, and TM7. These alignments were used with the standard homology modeling tools in the Quanta program (Accelrys, Princeton, NJ) to construct the seven helical bundle domains of the 5-HT₆ receptors.

The extracellular loop regions were subsequently added using a procedure developed in house, which makes use of a combined distance-geometry sampling and molecular-dynamics simulation (Blaney et al., 2001). The final rat and human receptor models were generated in a similar manner. Each model was optimized fully (500 steps of steepest descent minimization followed by adopted basis Newton-Raphson methods for 5000 steps) with the CHARMM force field (Accelrys) using helical distance constraints to maintain the backbone hydrogen bonds of the helix bundle.

The diverse ligands under study (Fig. 1) all contain a basic positively charged center, and this was therefore assumed to interact with the highly conserved aspartate residue Asp106 on TM3 (see *Discussion*). All of the ligand molecules used in this study were initially constructed using the builder options within the Spartan program (Wavefunction Inc., Irvine, CA) and were further optimized at the semiempirical AM1 level using the Vamp program (Accelrys). Some dihedral constraints were applied to maintain planarity, such as at the sulfonamide bonds, where appropriate. The resultant structures were then used to calculate ab initio charges for subsequent docking experiments. Natural atomic orbital charges were the ones of choice, and these were calculated with the use of Spartan using a 3-21G* basis set. All compounds were docked manually into the receptor models using a variety of low-energy conformations of the ligand. Adjustments of the protein side chains were made as necessary, always ensuring that these side chains were only in allowed rotameric states. Again, full optimization of the receptor-ligand complexes was performed using CHARMM; the only constraints were those that maintained the hydrogen-bonding pattern of the helical bundle. This procedure thus allows for the full relaxation of both the ligand and the whole protein, which is not possible with automated docking procedures. In all cases, several binding orientations were found to be possible.

Results

Distribution of 5-HT₆ Receptors in Different Species.

[¹²⁵I]SB-258585, a high-affinity and selective 5-HT₆ receptor radioligand (Hirst et al., 2000), was used to compare receptor protein levels in different regions of rat, mouse, and human brains. Within the rat central nervous system, the highest levels of specific binding were observed in the striatum and nucleus accumbens (24,600 ± 1600 and 17,900 ± 1700 cpm/mg protein, respectively) (Fig. 2A). Specific binding levels were 5-fold lower in cerebral cortex and thalamus and 8-fold lower in hippocampus and cerebellum (Fig. 2A). These data were determined using a single concentration of [¹²⁵I]SB-258585 (0.1 nM). However, a *B*_{max} value (the concentration of receptors in a tissue) can be estimated by calculating the receptor occupancy using the previously determined affinity of this radioligand at the native rat receptor (2.8 nM) (Hirst et al., 2000). For the rat striatum, this equates to 185 fmol/mg protein, a number which agrees closely with the value determined previously using full saturation and Scatchard analysis (173 fmol/mg protein) (Hirst et al., 2000). In the homogenates from three separate human patients, the highest levels were seen in the caudate nucleus and putamen (52,400 ± 3800 and 52,300 ± 3000, respectively) (Fig. 2B), suggesting an even distribution of this receptor subtype throughout the dorsal striatum. Specific binding levels in the nucleus accumbens were 28,800 ± 3800 cpm/mg protein, and substantially lower levels were detected in globus pallidus (7250 ± 60 cpm/mg protein), cerebral cortex (5170 ± 300 cpm/mg protein), hippocampus (3200 ± 95 cpm/mg protein), thalamus (2700 ± 270 cpm/mg protein), and cerebellum (2800 ± 650 cpm/mg protein) (Fig. 2B). In a manner similar to that described above, a *B*_{max} value can be estimated [the previously determined affinity of the radioligand in human caudate was 1.3 nM (Hirst et al., 2000)], and for the dorsal striatum this equates to 170 fmol/mg protein. In contrast, there was only a very low level (< 20 fmol/mg protein) of specific binding in the mouse brain regions and a

TABLE 1
TaqMan and site-directed mutagenesis (SDM) primers

Primer Direction	Primer Sequence	Nucleotides (from start codon)
TaqMan Primers (human 5-HT₆)		
Sense	5'-AGGCCTCTTCGATGTCCTCA-3'	897-916
Probe	5'-ATGGCTGGGTTACTGTAAACAGCACCATGAA-3'	918-947
Antisense	5'-CGCATGAAGAGTGGGTAGATGAT-3'	952-974
TaqMan Primers (rat and mouse 5-HT₆)		
Sense	5'-GCTGCGCAACACGTCTAACTTC-3'	168-189
Probe	5'-CTGGTGTGCTCTTCACGTCCGAC-3'	193-216
Antisense	5'-CACCACCAACCCACCATC-3'	219-237
TaqMan Primers (human GAPDH)		
Sense	5'-GGAAGCTCACTGGCATGGC-3'	677-695
Probe	5'-CCCCACTGCGCAACGTGTCAGTG-3'	705-726
Antisense	5'-TAGACGGCAGGTCAAGTCCA-3'	728-747
TaqMan Primers (rat GAPDH)		
Sense	5'-GAACATCATCCCTGCATCCA-3'	606-625
Probe	5'-CTTGCCACAGCCTTGGCAGC-3'	631-651
Antisense	5'-CCAGTGAGCTTCCCGTTCA-3'	665-683
SDM Primers (mouse 5-HT₆)		
S175P	5'-CTGGGCAAGCTCGAACACCCGCCCCGGGCCAGTGCCGC-3'	505-543
R181M	5'-CCGGGCCAGTGTCATGCTATTGGCCAGCCTGCC-3'	529-560
Y188F	5'-CTATTGGCCAGCTGCCTTTTGTCTCTGTCGTCGCGC-3'	544-583
S277G	5'-CTCGGCATCTGCTGGGCATGTTCTTTGTACC-3'	814-846
S290N	5'-TGCCCTTCTTTGTGGCAACATAGCTCAGGCCG-3'	851-883
SDM Primers (rat 5-HT₆)		
R188Y	5'-TATTGGCCAGCCTGCCTTATGTCCTCGTGG-3'	545-574

notable lack of enrichment of 5-HT₆ receptors in the striatum (Fig. 2C).

5-HT₆ receptor mRNA levels were measured in pooled

RNA samples from discrete rat, human, and mouse brain regions by TaqMan RT-PCR. In the rat brain, 5-HT₆ receptor mRNA expression was highest in the nucleus accumbens and striatum. Levels were approximately 9-fold lower in the amygdala and cerebral cortex and approximately 20-fold lower in the hippocampus, hypothalamus, and thalamus (Fig. 3A). No 5-HT₆ receptor mRNA was detected in rat cerebellum, medulla oblongata, pons, dorsal root ganglia, and spinal cord (Fig. 3A). In close agreement with the above data, human 5-HT₆ receptor mRNA expression was 6- to 10-fold higher in caudate nucleus, putamen, and nucleus accumbens than in cerebral cortex and hippocampus (Fig. 3B). Lower levels were also detectable in the amygdala, hypothalamus, and thalamus (Fig. 3B). No 5-HT₆ mRNA was detected in any of the following human peripheral tissues: heart, liver, lung, skeletal muscle, kidney, pancreas, spleen, small intestine, placenta, testis, stomach, prostate, or uterus (data not shown). In keeping with the radioligand binding studies, the TaqMan RT-PCR reveals extremely low levels of 5-HT₆ receptor mRNA in mouse brain (Fig. 3C). Furthermore, there was no enrichment of the mRNA in the mouse striatum. TaqMan RT-PCR was also undertaken to determine the levels of dopamine D₂ receptor mRNA. Enrichment of D₂ receptor mRNA was detected in rat and mouse striata (data not shown). Furthermore, [³H]spiperone binding, performed on the same samples used for [¹²⁵I]SB-258585 binding, showed a clear enrichment of specific binding for this D₂-selective radioligand in both rat and mouse striata (data not shown).

Pharmacological Profile of Recombinant 5-HT₆ Receptors from Different Species. After observing such a marked difference in the distribution pattern and relative expression level between rat and mouse 5-HT₆ receptors, we undertook experiments to investigate their pharmacology. This work was performed on recombinant receptors because the extremely low levels of specific binding of the selective radioligand [¹²⁵I]SB-258585 in mouse brain did not allow for competition binding experiments. After a number of preliminary experiments, [³H]LSD was used in preference to [¹²⁵I]SB-258585 because the affinity of [³H]LSD was not significantly different between species (1.5 ± 0.1 , 1.8 ± 0.3 , and 1.9 ± 0.2 nM for human, rat, and mouse, respectively). The relative level of expression of 5-HT₆ receptors from different species when transiently transfected in HEK 293 cells was similar (measured by radioligand binding) (data not shown). All of the transiently expressed wild-type receptors were functional, eliciting dose-dependent increases in cAMP levels when exposed to a 5-HT concentration range with pEC₅₀ values of 7.72 ± 0.04 and 7.85 ± 0.08 for rat and mouse, respectively. Consistent with the similar expression levels of the receptors described above, the E_{max} (maximal response) was $360 \pm 35\%$ and $340 \pm 37\%$ of basal levels for rat and mouse, respectively. Basal cAMP levels in the transiently transfected HEK 293 cells expressing either receptor were 60 to 80 pmol/ml.

Using competition binding analysis, we compared the affinity of a range of serotonergic agonists and antagonists and 5-HT₆ receptor-selective antagonists. 5-HT affinities differ slightly between the species (Fig. 4A and Table 2), and LSD has similar affinity at the 5-HT₆ receptor for all three species (Fig. 4B and Table 2). In contrast, there was a significant ($p < 0.01$) 24- and <1900-fold decrease in the affinity of the selective 5-HT₆ receptor antagonists SB-357134 and Ro 04-

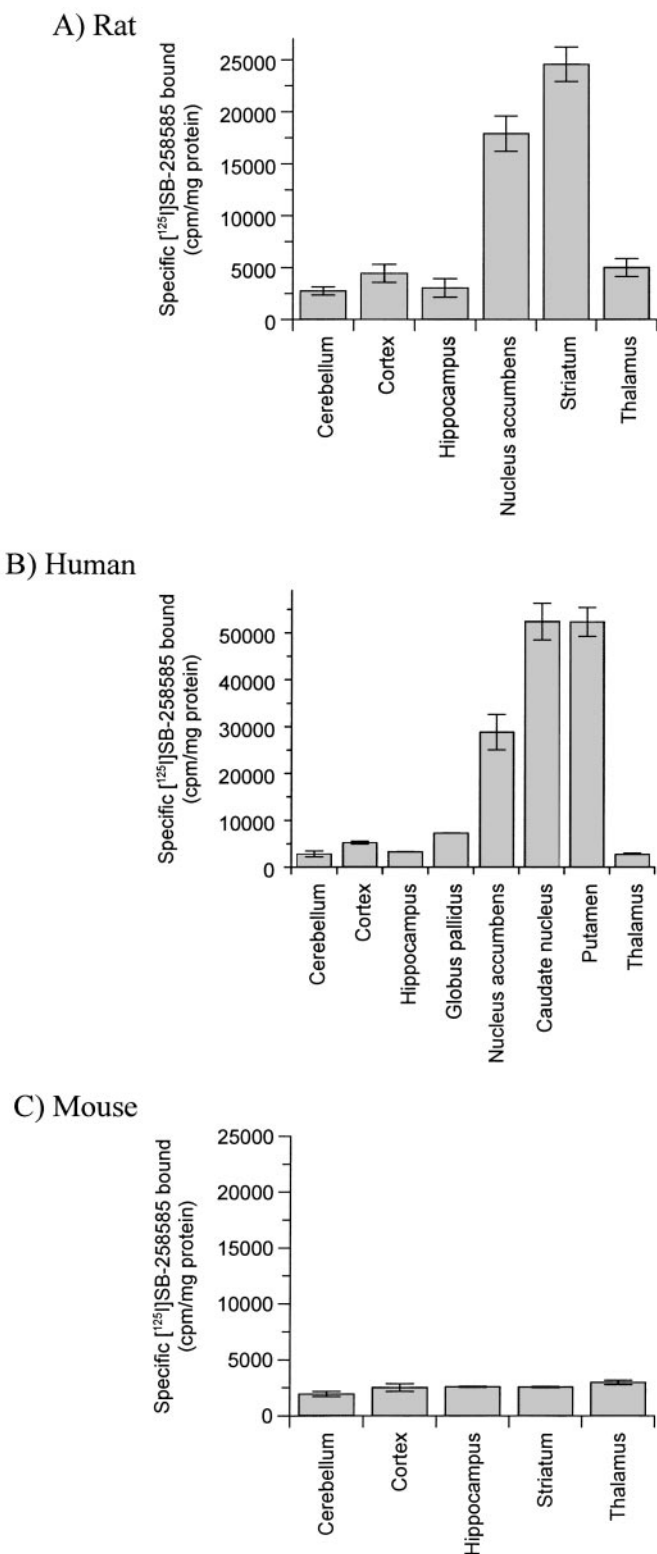


Fig. 2. Specific binding of 0.1 nM [¹²⁵I]SB-258585 to membrane homogenates derived from discrete rat (A), human (B), and mouse (C) brain regions. Nonspecific binding was defined in the presence of 10 μ M methiothepin. Data are expressed as the mean value \pm S.E. mean of at least three separate experiments.

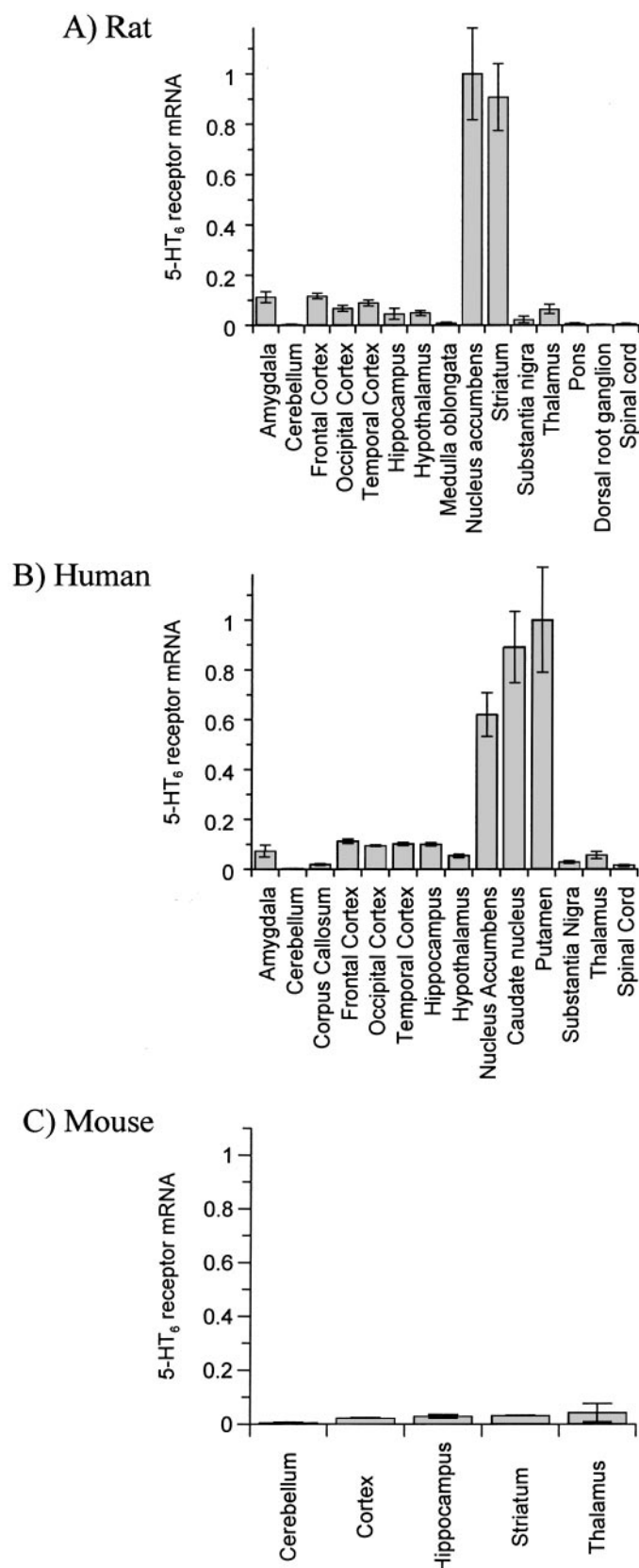


Fig. 3. Quantitative TaqMan RT-PCR determination of 5-HT₆ receptor mRNA levels in various rat (A), human (B), and mouse (C) brain regions. Primer sequences are shown in Table 1. Data are normalized to the housekeeping gene GAPDH and expressed as arbitrary units on a scale from 0 to 1. Data are expressed as the mean value \pm S.E. mean of at least three separate experiments.

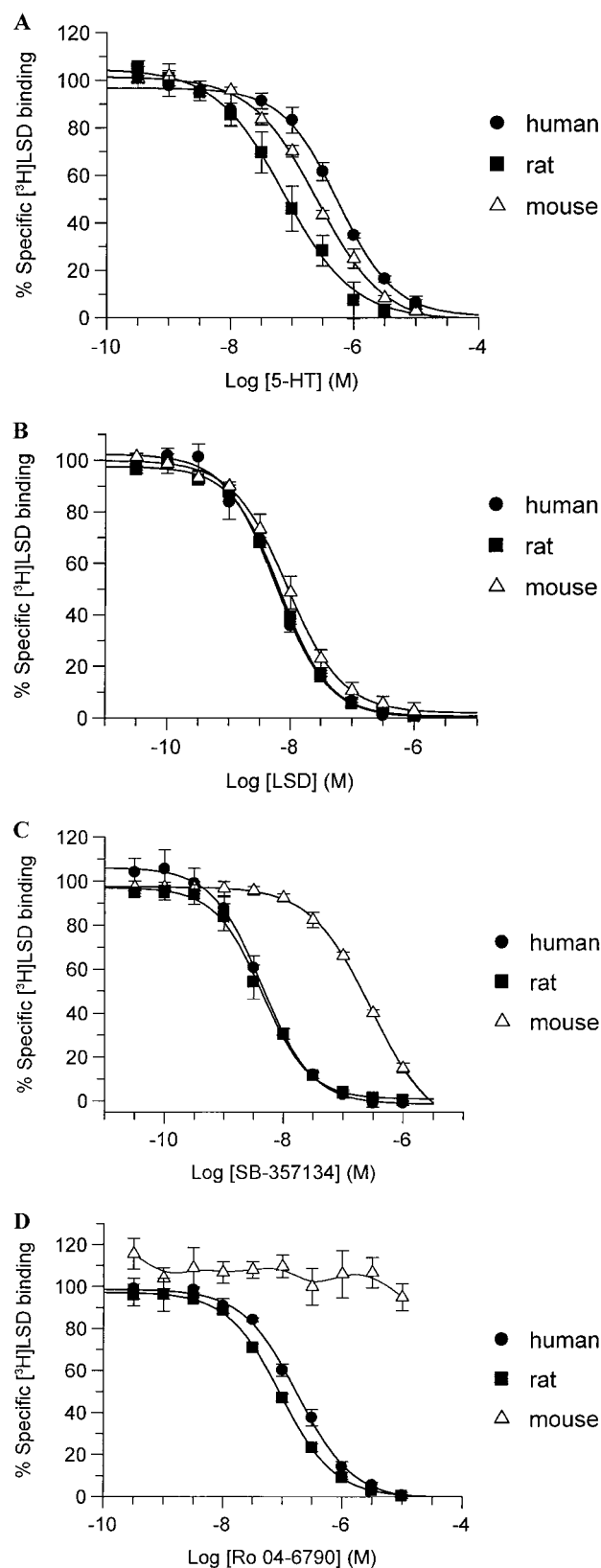


Fig. 4. Competition binding analysis of 5-HT (A), LSD (B), SB-357134 (C), and Ro 04-6790 (D) at human, rat, and mouse 5-HT₆ receptors transiently expressed in HEK 293 cells. [³H]LSD was used at a final concentration of 2 nM, and nonspecific binding was defined in the presence of 10 μ M methiothepin. Data points represent the means \pm S.E. mean of at least three separate experiments. Average pK_i values for these compounds and others tested are shown in Table 2.

6790, respectively, at the mouse receptor compared with rat and human (Fig. 4, C and D; Table 2). The decrease in affinity for the mouse 5-HT₆ receptor was less pronounced with other selective 5-HT₆ receptor antagonists, such as SB-258585, SB-214111, and SB-271046, whereas there was no significant difference in affinity at rat and mouse receptors with SB-258510 (Table 2). Conversely, mianserin and sumatriptan showed 10- and 6-fold increases, respectively, in binding affinity at the mouse receptor compared with the rat and human 5-HT₆ receptors. Data from the 14 compounds studied are shown in Fig. 5, in which a plot of pK_i values determined in competition binding experiments give a correlation coefficient (r) of 0.99 (human versus rat) and 0.66 (mouse versus rat).

Sequence Alignment of Mouse/Rat/Human 5-HT₆ Receptors Identified Four Amino Acids Possibly Responsible for the Observed Pharmacological Differences Between Species. To investigate the species-dependent pharmacological differences further, we used the Clustal W program to align the amino acid sequences of the mouse, rat, and human 5-HT₆ receptors and identified residues that differed between the three sequences. Because the species differences in the pharmacological profiles observed with recombinant receptors in the present study occurred predominantly between mouse and rat (the pharmacological profiles of the human and rat receptors were virtually identical), we concentrated specifically on residues that differed between mouse and both rat and human. In addition, we only studied residues that were predicted to be either within the extracellular domains or within the transmembrane regions, because these are the regions most likely to affect ligand binding. Using these criteria, we identified just four residues within the 5-HT₆ receptor sequence that differ between mouse and rat/human which might be responsible for the observed differences in pharmacology; in the mouse, these were serine 175 (S175) in the second extracellular loop (ECL2), tyrosine 188 (Tyr188) in TM5, and serine 277 (Ser277) and serine 290 (Ser290) in TM6 (Fig. 6A). In the rat and human 5-HT₆ sequences, these residues were identified as proline 175, phenylalanine 188, glycine 275, and asparagine 288, respectively (Fig. 6A). It is also worth noting that there is a two amino acid insertion in the mouse sequence in the third

intracellular loop and in the human in the C-terminal domain.

Investigation of the Residues Responsible for Species Differences by Site-Directed Mutagenesis and Radioligand Binding. The divergent residues in the mouse sequence were systematically mutated individually or in combination to investigate which of them contributed to the ligand binding and conferred the difference in pharmacological profile between the species. The binding affinities of a range of compounds used to define the pharmacological profile of wild-type and mutated mouse receptors are shown in Table 3.

The pharmacological profile of the S175P mutation was not significantly different from the wild-type mouse profile. In contrast, the Y188F in TM5 mutation resulted in marked changes in the profile of the mouse receptor; notably, the affinity of Ro 04-6790, SB-357134, SB-258585, and SB-271046 increased from <4, 7.21, 7.95, and 8.91 to 6.35, 8.64, 8.55, and 9.32, respectively. LSD, 5-HT, mianserin, and methiothepin affinities were unchanged compared with wild-type mouse. Changing S277G in TM6 modified the affinity of a number of compounds: LSD affinity increased compared with wild-type, but 5-HT, mianserin, and SB-271046 affinities decreased, and pK_i values for other compounds were unchanged. The S290N mutation increased the affinity of Ro 04-6790, but it resulted in a significant 8-fold decrease in mianserin affinity. The profile of compound affinity at the S175P/Y188F and Y188F/S277G double mutation is no different from the Y188F single mutant, except for a decrease in SB-271046 affinity in the former and a decrease in mianserin affinity in the latter. Similarly, the S277G/S290N double mutation does not show any additional changes to those seen in the S290N single mutant. However, the Y188F/S290N double mutant does show some additional increases in affinity of SB-357134 and Ro 04-6790 and a decrease in affinity for mianserin above that seen in both of the corresponding single mutants. The triple and quadruple mutations, predictably, almost completely modified the mouse pharmacological profile to that of the rat, with the exception of a small but significant ($p < 0.05$) decrease in SB-357134 and Ro 04-6790 affinity. A single mutation to the rat sequence to introduce a tyrosine residue instead of the conserved phenylalanine at

TABLE 2

Pharmacological profile of recombinant rat, human, and mouse 5-HT₆ receptor

Receptors were transiently expressed in HEK 293 cells, and compound affinity for the receptors was determined in competition binding assays using [³H]LSD. Data are expressed as the mean pK_i value \pm S.E. mean of at least three separate experiments.

Compound	pK_i		
	Human 5-HT ₆ Receptor	Rat 5-HT ₆ Receptor	Mouse 5-HT ₆ Receptor
5-HT	6.88 \pm 0.02	7.10 \pm 0.07	7.02 \pm 0.04
5-MeO-T	7.16 \pm 0.03	7.65 \pm 0.17	7.63 \pm 0.09
LSD	8.64 \pm 0.01	8.58 \pm 0.03	8.55 \pm 0.03
Clozapine	7.84 \pm 0.07	7.96 \pm 0.16	8.19 \pm 0.08
Methiothepin	8.85 \pm 0.07	8.98 \pm 0.13	9.25 \pm 0.10
Mianserin	7.09 \pm 0.03	7.40 \pm 0.20	8.49 \pm 0.08**
Amitriptyline	6.85 \pm 0.04	6.74 \pm 0.05	7.05 \pm 0.10
Sumatriptan	4.52 \pm 0.20	4.46 \pm 0.02	5.25 \pm 0.05**
SB-258510	8.99 \pm 0.06	9.12 \pm 0.08	9.00 \pm 0.04
SB-271046	9.09 \pm 0.04	9.15 \pm 0.02	8.91 \pm 0.02**
SB-357134	8.59 \pm 0.03	8.85 \pm 0.08	7.21 \pm 0.04**
SB-214111	8.55 \pm 0.05	8.32 \pm 0.08	7.64 \pm 0.07**
SB-258585	8.74 \pm 0.01	8.64 \pm 0.07	7.95 \pm 0.05**
Ro 04-6790	7.29 \pm 0.01	7.54 \pm 0.05	< 4**

** $p < 0.01$.

position 188 was undertaken, and the data from competition binding experiments confirmed that this mutation significantly decreased the affinity for all of the selective 5-HT₆ receptor antagonists but did not alter the affinity of mianserin or methiothepin.

5-HT₆ Receptor Modeling and Ligand Docking. A combination of the analysis of sequence conservation between the human and rodent 5-HT receptors, the Kyte-Doolittle hydropathic analysis, and the known structure of bovine rhodopsin was used to predict the transmembrane domains of the mouse 5-HT₆ receptor. This is shown schematically in Fig. 6B. It was noted above that the major differences in the pharmacological profiles of the 5-HT₆ receptors between species arise as a result of the Y188F and, to a lesser extent, S290N mutations (Table 3). Amino acid side chains are well known to adopt discrete dihedral angles, commonly known as rotamers. A statistical evaluation of these dihedral angles observed among known crystal struc-

tures of proteins has led to the development of rotamer libraries, which tabulate the preferred conformations of the different side chains and their relevant populations (Dunbrack, 2002). Tyrosine, for example, can adopt three staggered conformations around the C α -C β bond (χ_1 angles). In the model of the mouse 5-HT₆ receptor, tyrosine Y188 was found to prefer the less favorable *gauche* + rotameric state. In doing so, however, it formed a strong hydrogen bond with Ser290 (Fig. 7). Mutation of the tyrosine to phenylalanine abolishes this hydrogen bond, and as a result, the phenylalanine adopts the more favored *trans* conformation. Thus, the binding pocket is predicted to be different in the two species, and it seems reasonable to assume that differences in the interaction of the ligands with this tyrosine/phenylalanine might account for some of the observed effects of the mutations.

Ro 04-6790. One of the most striking selective compounds was the Roche compound Ro 04-6790. Although this compound is not as basic as most of the other ligands, protonation of this compound is possible. Ab initio calculations were used to determine which was the more favored basic site. Protonation can occur in theory at either of the pyrimidine nitrogens. Ab initio calculations (3-21G* basis set) and subsequent population analysis using either Mulliken or natural atomic orbital charges did little to distinguish between the two sites (Table 4). Electrostatic potential calculations using the same basis set, however, did suggest that a greater negative potential at N3 would favor protonation at this site. The individual protonated species (at N1 and N3) were then optimized at this level, and it was found that the N3 protomer was more stable by some 5.8 kcal/mol (Table 4). This protonated isomer was therefore docked into the mouse and rat receptor models. In the rat, the protonated pyrimidine clearly forms a bidentate interaction between the TM3 aspartate and the hydrogens of N3 and its adjacent 2-methylamino group. The other 6-methylamino NH can form a hydrogen bond with the oxygen of threonine T306 on TM7. The pyrimidine ring itself sits in a well-defined aromatic π -stacking orientation with Phe284, whereas its pendant substituents at the 2 and 6 positions form hydrophobic interactions with tryptophan W281 and with Phe302 on TM7. The model predicts that both sulfonamide oxygens can form hydrogen bonds, one with the important Asn288 and the other with Gln216, which is adjacent to the disulfide-forming cysteine in extracellular loop 2. The 4-aminophenyl ring sits in close proximity to the crucial Phe188 with the amino hydrogens, making a good electrostatic interaction with the ring (see Fig. 8A for a depiction of this binding mode). On docking Ro 04-6790 into the mouse receptor, the different orientation of the equivalent Tyr188 resulted in the ligand sitting considerably lower in the binding pocket. The 4-aminophenyl ring was no longer able to interact as favorably with the aromatic ring of Tyr188, and no hydrogen bonds were formed with the sulfonamide oxygens or between the methylamino NH and Thr308. The pyrimidine ring did sit in an aromatic pocket formed by Trp283, Phe286, and Tyr312, but this was clearly not enough to compensate for the loss of the other interactions. The mutation of Y188F allows the ligand to move higher in the pocket, allowing it to reform two of the hydrogen bonds and restoring the aromatic interaction with Phe188. It was seen also that the S290N mutation can cause a partial restoration of activity. This is readily explained by

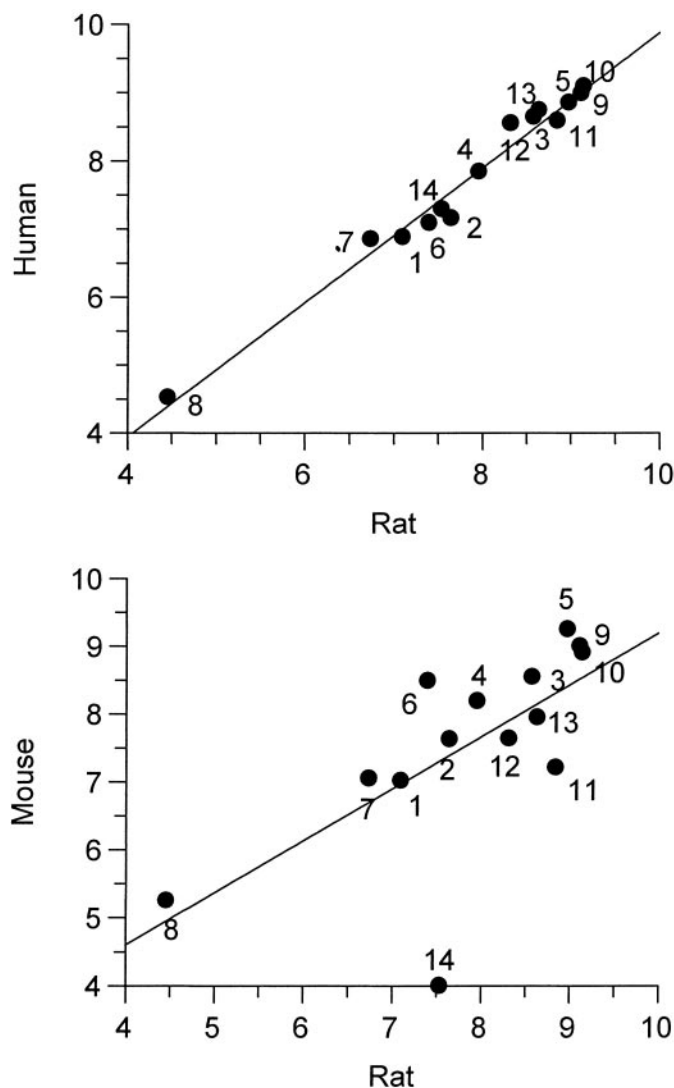


Fig. 5. Correlation plot of pK_i values for 14 compounds inhibiting [³H]LSD binding at human, rat, or mouse 5-HT₆ receptors transiently expressed in HEK 293 cells. A correlation coefficient (*r*) of 0.99 (human versus rat, slope = 0.99) (A) and 0.66 (mouse versus rat, slope 0.77) (B) was obtained. 1, 5-HT; 2, 5-MeO-T; 3, LSD; 4, clozapine; 5, methiothepin; 6, mianserin; 7, amitriptyline; 8, sumatriptan; 9, SB-258510; 10, SB-271046; 11, SB-357134; 12, SB-214111; 13, SB-258585; 14, Ro 04-6790.

the reforming of a strong hydrogen bond between the asparagine and one of the sulfonamide oxygens. As observed, the double mutation Y188F/S290N would be expected to restore most of the interactions which were lost in the mouse wild-type receptor.

Methiothepin and LSD. From the docking of Ro 04-6790, our attention turned to the nonselective ligands methiothepin and LSD. Both compounds are presumed to form salt bridges between their basic protonated nitrogens and Asp106. As shown in Fig. 8B, in the rat receptor, the docked LSD ligand had its tetracyclic ring system in a hydrophobic pocket between TM3 and TM6, lined by Trp281, Phe284 and Phe285, Val107, and Cys110. The indole NH hydrogen bonds to Thr196 (TM5), whereas the amide carbonyl forms similar interactions with Thr306 (TM7) and Gln179 (ECL2). These interactions are all broadly similar in the mouse receptor docking model, although the hydrogen bond to Thr196 is weaker. A main difference between the two models is in the interaction with the TM5 aromatic residue. The rat Phe188 points toward the face of the indole ring, forming a T-type aromatic interaction with it. The equivalent Tyr188 in the

mouse also forms a T-type interaction, only in this case it is the indole that is oriented toward the face of the amino acid. The overall predicted binding interactions are therefore similar in energy, which is reflected in the lack of selectivity of LSD. The smaller methiothepin ligand resides in both receptors in the same hydrophobic pocket formed by W281r/283m, Y310r/312m, Val107, and F283r/285m and F284r/286m. The importance of these aromatic residues in TMs 6 and 7 has been highlighted previously by the mutagenesis work of Roth et al. (1997), who studied the effects of mutation of these residues on agonist response in the 5-HT_{2A} receptor. The TM5 aromatic Phe188 residue in the rat model is in the vicinity of the thiopin sulfur without forming any real interaction. The equivalent Tyr188 in the mouse is not particularly close to the ligand.

Sulfonamide Analogs. With all of the sulfonamide analogs (SB-357134, SB-214111, SB-258585, SB-258510, and SB-271046), we assumed that the primary binding interaction was between the nonanilino piperazine nitrogen and the TM3 Asp106. With SB-357134, the hydrogen bond between Tyr188 and Ser290 in the mouse receptor needs to be broken

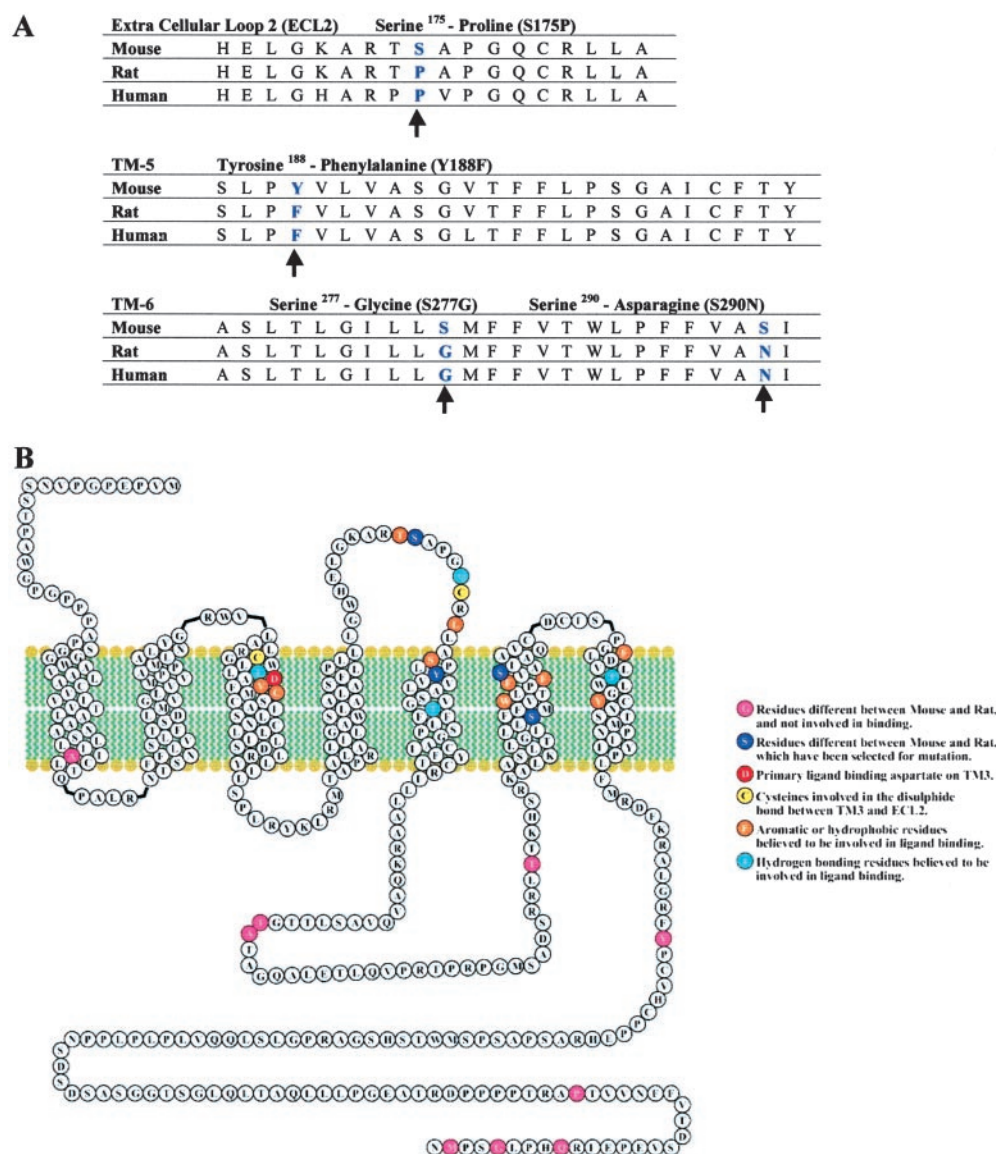


Fig. 6. A, alignment of the amino acid sequences from the second extracellular loop and the fifth and sixth putative transmembrane domains of mouse, rat, and human 5-HT₆ receptors. The amino acids that are distinct in the mouse, compared with rat and human sequences, and were selected for mutagenesis studies are shown by arrows. B, a schematic diagram of the mouse 5-HT₆ receptor showing the TM and loop topology. A combination of the analysis of sequence conservation between the human and rodent 5-HT receptors, the Kyte-Doolittle hydrophobic analysis, and the known structure of bovine rhodopsin was used to predict the transmembrane domains of the mouse 5-HT₆ receptor. Residues that are involved in binding or that are different between the mouse and rat sequences are highlighted. The four residues that were mutated are shown in dark blue. Because of the two-residue insertion in the mouse third intracellular loop, rat and human residues from TM6 onward will have different numbers. In the text, such differences are named, for example, S290m/N288rh, which means that for the serine 290 in the mouse sequence, the equivalent residue is an asparagine at position 288 in the rat and human sequences.

TABLE 3

Effect of point mutations of the mouse and rat 5-HT₆ receptors on binding affinity of a range of selective and nonselective 5-HT₆ receptor ligands

Receptors were transiently expressed in HEK 293 cells, and compound affinity for the receptors was determined in competition binding assays using [³H]LSD. The affinities of a range of compounds at the wild-type (wt) rat and mouse receptors in addition to single, double, triple, and quadruple mutations are shown (with the exception of the final column, all mutations were performed on the mouse sequence). Data are expressed as the mean pK_i value ± S.E. mean of at least three separate experiments. For clarity, statistical probability (*p*) values have been excluded. Key differences are described under Results.

Compound	Rat-wt	Mouse-wt	S175P	Y188F	S277G	S290N	S175P / Y188F	Y188F / S277G	Y188F / S290N	S277G / S290N	Y188F / S277G / S290N	S175P / Y188F / S277G / S290N	Rat F188Y
5-HT	7.10 ± 0.07	7.02 ± 0.04	6.95 ± 0.19	7.17 ± 0.04	6.77 ± 0.04	7.35 ± 0.27	7.18 ± 0.19	7.10 ± 0.07	7.18 ± 0.03	7.30 ± 0.15	6.96 ± 0.07	7.28 ± 0.01	7.44 ± 0.03
LSD	8.58 ± 0.03	8.55 ± 0.03	8.67 ± 0.03	8.67 ± 0.09	8.72 ± 0.04	8.77 ± 0.05	8.71 ± 0.03	8.61 ± 0.02	8.73 ± 0.04	8.60 ± 0.01	8.82 ± 0.01	8.74 ± 0.04	8.62 ± 0.02
Methiothepin	8.98 ± 0.13	9.25 ± 0.06	9.09 ± 0.06	9.23 ± 0.05	9.27 ± 0.09	9.01 ± 0.11	9.18 ± 0.01	9.15 ± 0.05	8.77 ± 0.08	9.02 ± 0.07	8.56 ± 0.17	8.75 ± 0.07	8.95 ± 0.05
Mianserin	7.40 ± 0.20	8.49 ± 0.08	8.34 ± 0.11	8.48 ± 0.15	8.10 ± 0.12	7.59 ± 0.17	8.31 ± 0.01	7.79 ± 0.21	7.60 ± 0.06	7.47 ± 0.10	7.36 ± 0.05	7.31 ± 0.03	7.39 ± 0.05
SB-258510	9.12 ± 0.08	9.00 ± 0.04	8.67 ± 0.05	9.02 ± 0.06	9.07 ± 0.14	9.07 ± 0.22	8.84 ± 0.19	9.12 ± 0.16	8.98 ± 0.05	8.90 ± 0.05	9.29 ± 0.17	9.07 ± 0.07	8.66 ± 0.09
SB-271046	9.15 ± 0.02	8.91 ± 0.02	8.55 ± 0.12	9.32 ± 0.07	8.57 ± 0.19	8.97 ± 0.11	8.94 ± 0.14	9.19 ± 0.24	9.05 ± 0.15	8.81 ± 0.12	9.13 ± 0.18	9.16 ± 0.05	8.57 ± 0.07
SB-357134	8.85 ± 0.08	7.21 ± 0.04	7.00 ± 0.06	8.64 ± 0.14	7.27 ± 0.08	7.42 ± 0.18	8.41 ± 0.02	8.66 ± 0.12	8.89 ± 0.29	7.43 ± 0.07	8.47 ± 0.20	8.59 ± 0.05	7.13 ± 0.02
SB-258585	8.64 ± 0.07	7.95 ± 0.05	7.75 ± 0.03	8.55 ± 0.10	8.01 ± 0.07	8.10 ± 0.16	8.35 ± 0.10	8.52 ± 0.20	8.76 ± 0.06	8.09 ± 0.03	8.62 ± 0.06	8.82 ± 0.09	7.99 ± 0.07
Ro 04-6790	7.54 ± 0.05	<4	<4	6.35 ± 0.12	<4	5.75 ± 0.17	6.14 ± 0.09	6.32 ± 0.07	7.14 ± 0.05	5.59 ± 0.17	7.23 ± 0.04	7.34 ± 0.03	<4

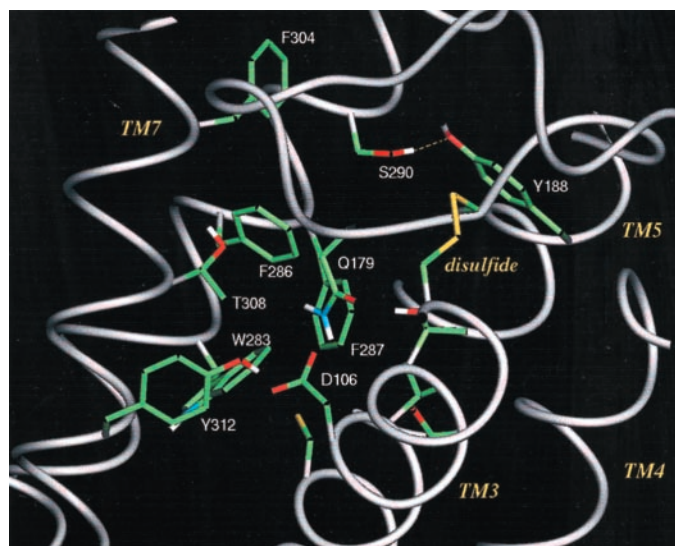


Fig. 7. The binding pocket of the mouse 5-HT₆ receptor. Most of the residues that are believed to be involved in binding are shown here. Primary binding of the ligand basic centers occurs to Asp106. The yellow line toward the top of the figure highlights the strong hydrogen bond between Tyr188 and Ser290.

to accommodate the sulfonamide group. This results in the formation of an alternative hydrogen bond between the sulfonamide NH and Ser290. However, by moving the TM5 tyrosine to the *trans* rotameric state, it forms an unfavorable dipole-dipole interaction with the methoxyphenyl ring of the ligand. Furthermore, the ligand is pushed into a less favorable geometry for the salt bridge with the TM3 aspartate. In the rat receptor, however, the Asn288 now forms a strong hydrogen bond with one of the sulfonamide oxygens, moving the ligand deeper into the pocket where it can form a more favorable salt bridge with Asp106 and a π - π stacking with phenylalanine F188 (see Fig. 8C). The mouse Y188F mutation removes the unfavorable dipole-dipole interaction, thus allowing the ligand to reform the π - π stacking and to improve its salt-bridge geometry. The opposite is expected and observed with the F188Y mutation in the rat receptor. The different pockets occupied by the ligand in the two receptors is also reflected in the position of the dibromophenyl ring. In the mouse, this sits in a hydrophobic pocket between Phe304 and Thr174 in ECL2. In the rat model, this is in an alternative pocket of ECL2 lying between Leu182, Ser185, and Thr174.

By reversing the sulfonamide linkage, such as in the compounds SB-258510 and SB-271046, docking studies showed that the ligand adopts a position in which it can form a good π - π stacking with either the TM5 tyrosine or phenylalanine. Although the Ser290 in the mouse receptor has to break the hydrogen bond to Tyr188 to do so, it forms one with one of the sulfonamide oxygens with no net change in energy. The reversed sulfonamides were therefore predicted not to exhibit any selectivity between the species.

Mianserin and Analogs. In this study, mianserin is unique in exhibiting a significant 10-fold increase in binding affinity for the mouse receptor over the rat. Furthermore, the results in Table 3 suggest that this is not caused by the differences in the aromatic pocket from the Y188F change but rather by the influence of Asn290 in the rat receptor. Some years ago, before the advent of receptor modeling, we

were involved in the design of novel analogs of mianserin with improved receptor selectivity (Orlek et al., 1993). It was recognized at the time that the mianserin ring system can exist in four distinct conformations, and it was likely that differing conformations were responsible for its activity at various aminergic receptors. Generally, dibenzapine ring systems can flip between two ring conformations around the central 7-membered ring. In the case of mianserin, this places the bridgehead azepine ring hydrogen either *syn* or *anti* to one of the opposite methylene hydrogens. Furthermore, the presence of the adjacent bridgehead nitrogen means that the ring junction itself can readily interconvert by nitrogen inversion between *cis* and *trans* forms. The relative energies of these forms were calculated after geometry optimization at the molecular mechanics, AM1 semiempirical, and ab initio 3-21G* levels. In mianserin, it is clear from the calculations that the *trans-anti* conformer is the preferred form. Indeed, for mianserin, this is the conformation found both by crystallography (Van Meerssche and Declercq, 1983) and by solution NMR (Funke and Carel, 1982). The *cis-anti* conformer can clearly be ruled out because under normal optimization conditions, it inverts to an alternative conformation and is by far the highest conformer in energy. The two other conformations, i.e., the *cis-syn* and the *trans-syn*, are intermediate in energy.

Docking of mianserin in the *trans-anti* conformation to the mouse receptor model predicted that, in addition to the usual salt bridge between the piperazine nitrogen and Asp106, a π - π stacking occurred between Phe286 and one of the aromatic rings of the ligand, and an orthogonal aromatic-aromatic interaction occurred between Phe287 and the other ring. No other significant interactions were observed with this conformer. With the *cis-syn* conformer, however, Phe286 formed the more favorable orthogonal interaction with both rings of the ligand. Weaker orthogonal interactions could also be formed with Phe287 and Phe304 (TM7). Val107 also formed a highly favorable hydrophobic interaction (Fig. 9). Thr103 could hydrogen-bond to the bridgehead nitrogen. Thus the overall binding mode of mianserin in the mouse favors the *cis-syn* conformation. It is noteworthy that Tyr188 sits at the edge of the pocket with both ligand conformations and does not have any significant interactions. By adopting the alternate rotameric state as in the Phe188 of the rat and human receptors, there are still no significant interactions with either conformation of mianserin. This explains the lack of effect observed with the Y188F mutation. Replacement of Ser290 by Asn, on the other hand, results in a large steric

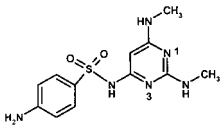
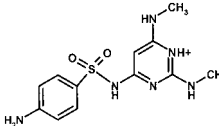
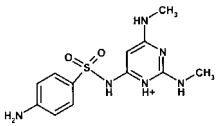
clash with the nearby aromatic ring of the ligand. This effect is the same with both conformations.

In the previously mentioned study of mianserin (Orlek et al., 1993), several ligands were synthesized with the aim of locking the conformation of the ring system. Energy optimizations, calculated before their syntheses, predicted that one of these, BRL-34849, clearly favored the *cis-syn* state by ~6 kcal over the *trans-anti* state. This was subsequently confirmed by X-ray crystallography and solution NMR (Orlek et al., 1993). BRL-34969, on the other hand, showed no clear preference for any single conformation. The *cis-anti* conformer was calculated at the ab initio level to be 2.5 kcal higher in energy than the other three states, which were essentially equal in energy. The solution NMR of BRL-34969 does show that it is predominantly in the *trans-anti* conformation, similar to mianserin itself (Orlek et al., 1993). We decided to look at the effects of the various mutants on these compounds to determine whether the proposed *cis-syn* conformation would be confirmed. The results are summarized in Table 5. As with mianserin, BRL-34849 shows a selectivity of approximately 10-fold over the human receptor. This would suggest that the *cis-syn* conformation, in which this ligand is "locked", is the preferred one for the mouse receptor. BRL-34969, which presumably can exist in an ensemble of alternative conformations, exhibits no selectivity for either wild-type or mutant receptors. As with mianserin, BRL-34849 shows a decrease with the S290N mutant, again reinforcing the proposed binding mode for the mianserin analogs. With mianserin docked in the *trans-anti* conformation, there is no expected steric clash between the ligand and asparagine N288 of the rat and human receptors. This explains the lack of effect with the S290N mutant on BRL-34969.

Discussion

The work reported in the present study was initiated by the striking observation that there were only very low levels of specific binding of the high-affinity 5-HT₆ receptor-selective radioligand [¹²⁵I]SB-258585 (Hirst et al., 2000) in the mouse brain. This is in stark contrast to the rat and human brain, which showed considerable binding of this radioligand to the nucleus accumbens and striatum, in agreement with previous studies that have described the distribution of the 5-HT₆ receptor protein by immunohistochemistry (Gerard et al., 1997; Hamon et al., 1998) and receptor autoradiography (East et al., 2002; Roberts et al., 2002).

TABLE 4
Calculated ab initio properties of the neutral and protonated states of Ro 04-6790

<div></div>			<div></div>			<div></div>		
Property			N1	N3	Relative HF Energy			
Electrostatic potential			−59.01	−65.72	0.0 kcal/mol			−5.84 kcal/mol
Mull. Chg			−0.30	−0.31				
NAO Chg			−0.30	−0.31				
ESP Chg			−0.85	−0.88				

Mull. Chg., Mulliken population charges; NAO Chg., natural atomic orbital charges; ESP Chg., electrostatic potential fitted point charges; HF, Hartree-Fock.

These observations were corroborated by the current TaqMan quantitative RT-PCR studies, in which we have demonstrated an enrichment of 5-HT₆ receptor mRNA in the nucleus accumbens and striatum compared with other brain regions in human and rat. These data are consistent with a

number of previous studies that have investigated 5-HT₆ receptor mRNA distribution in the rat brain by Northern blot analysis (Monsma et al., 1993; Ruat et al., 1993) and in situ hybridization (Ruat et al., 1993; Ward et al., 1995) and in human brain regions by Northern blot analysis (Kohen et al., 1996) and in situ hybridization (East et al., 2002). In keeping with the radioligand binding studies, we could only detect very low levels of 5-HT₆ receptor mRNA in mouse brain regions using the sensitive and quantitative technique of TaqMan RT-PCR and did not observe enrichment in the striatum. The low level of expression of 5-HT₆ receptors by mice was not a strain-specific phenomena, because we obtained identical results from two distinct strains of mice, C57/Bl6 and CD-1 (data not shown).

These results clearly demonstrate that the mouse is unique compared with rat, pig, and human, all of whom express relatively high levels of 5-HT₆ receptors, especially in the striatum (Hirst et al., 2000). Although the direct physiological implications of this are currently unknown, it does suggest that mice are not an ideal species in which to conduct behavioral or physiological experiments pertaining to 5-HT₆ receptor function. Interestingly, a 5-HT₆ receptor knockout mouse has been generated in which a preliminary report described increased anxiety in these animals (Tecott et al., 1998). However, more recent studies have failed to demonstrate anxiogenic effects of selective 5-HT₆ receptor antagonists in rats (Bentley et al., 1999; Routledge et al., 2000; Stean et al., 2002), making the interpretation of the knockout studies rather difficult.

Despite the low level of expression, the mouse receptor was cloned without difficulty using standard protocols, and the sequence we obtained was identical with that reported previously (Kohen et al., 2001). Transient expression in HEK 293 cells allowed us to investigate the pharmacological profile of the receptor, which was not undertaken previously by Kohen et al. (2001). Surprisingly, considering the high degree of sequence homology between rat and mouse 5-HT₆ receptors, in the present study we obtained a distinct pharmaco-

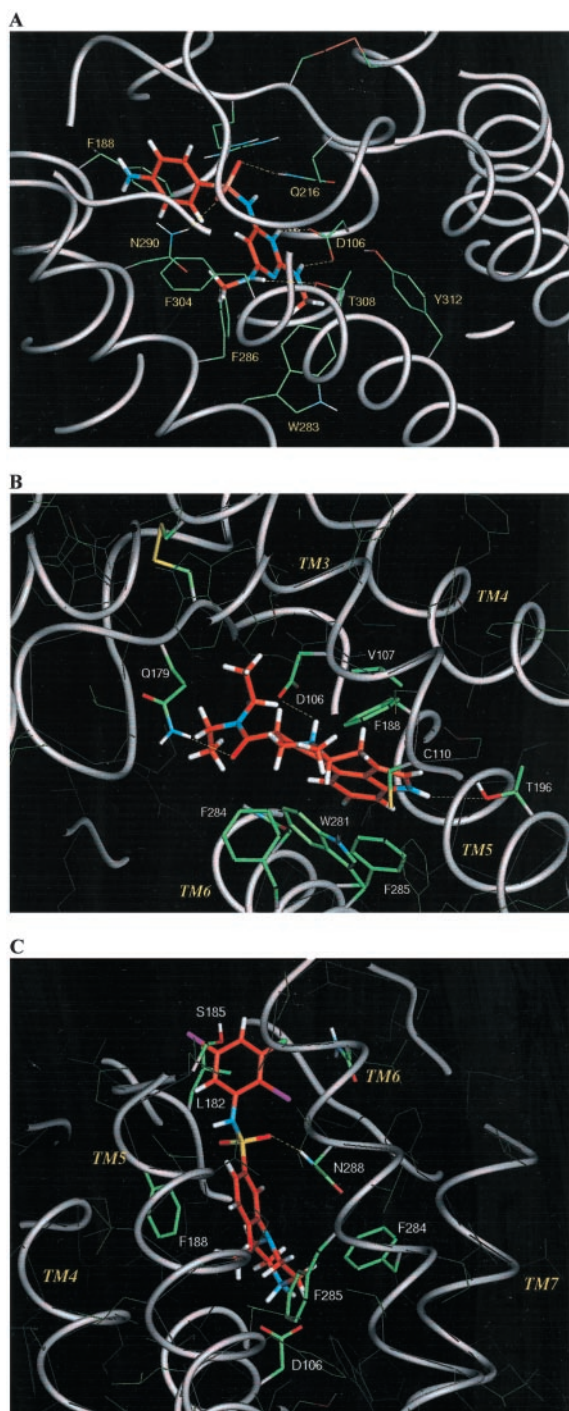


Fig. 8. Docking of ligands into the rat 5-HT₆ receptor. Most residues have been removed for clarity. A, docking of Ro 04-6790, the key hydrogen-bond interactions, is shown as broken yellow lines. B, docking of LSD, highlighting the main hydrogen-bond interactions, is shown as broken yellow lines. Note the coplanar stacking of Phe285 and the orthogonal aromatic interaction of Phe188 with the indole ring of the ligand. C, docking of SB-357134. The piperazine ring sits between Phe284 and Phe285. Note the strong hydrogen bond between Asn288 and the sulfonamide and the coplanar stacking of Phe188 with the methoxyphenyl ring.

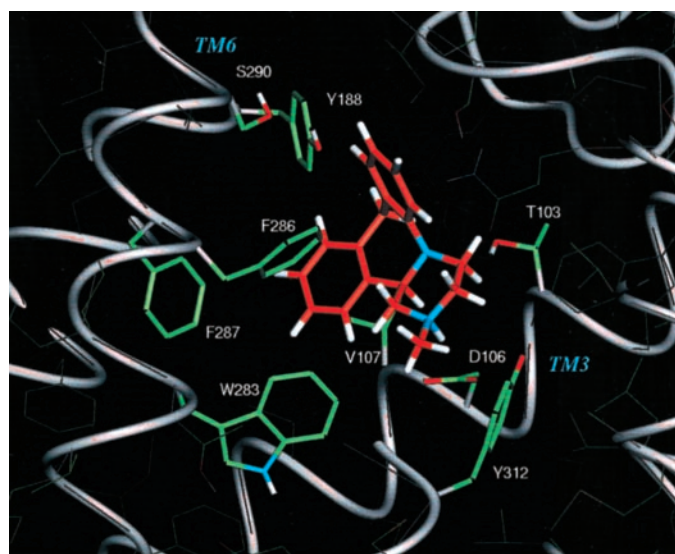


Fig. 9. Docking of *cis-syn* mianserin into the mouse 5-HT₆ receptor. Note the orthogonal aromatic interactions that Phe288 makes with both phenyl rings of the ligand. Tyr188 is not very close to the ligand, but Ser290 is quite close to the upper ring. Mutation of this residue to asparagine causes a steric clash with this ring.

TABLE 5

Effects of mutations on the affinity of mianserin and its analogs

Receptors were transiently expressed in HEK 293 cells, and compound affinity for the receptors was determined in competition binding assays using [³H]LSD. Data are expressed as the mean pK_i value ± S.E. mean of three separate experiments.

Compound	Human Wild-Type	Mouse Wild-Type	S175P	Y188F	S277G	S290N
Mianserin	7.10 ^a ± 0.09	8.49 ± 0.08	8.34 ± 0.11	8.48 ± 0.15	8.10 ± 0.12	7.59 ± 0.17
BRL-34849	6.78 ± 0.06	7.62 ± 0.02	7.68 ± 0.03	7.65 ± 0.02	7.51 ± 0.04	7.11 ± 0.08
BRL-34969	6.39 ± 0.05	6.61 ± 0.02	6.60 ± 0.06	6.67 ± 0.06	6.44 ± 0.09	6.44 ± 0.09

^a Affinity of mianserin at the rat wild-type receptor = 7.40.

logical profile for the mouse receptor compared with rat and human. We and others have previously shown that the rat and human receptors have a very similar profile (Boess et al., 1998; Hirst et al., 2000). The mouse profile was particularly interesting because the affinity of the nonselective agonists; 5-HT, 5-MeO-T, and LSD were not significantly different from the rat and human profiles. However, the affinity of some, but not all, previously described selective 5-HT₆ receptor antagonists were significantly decreased. Furthermore, the affinity of mianserin and sumatriptan were significantly increased. These observations led us to identify four residues, predicted to be toward the extracellular side of the receptor, which could be responsible for the observed differences in pharmacology: S175m/P175rh, Y188m/F188rh, S277m/G275rh, and S290m/N288rh. The four divergent residues in the mouse sequence were mutated individually or in combination to investigate their contribution to the ligand binding site, and this information was used in receptor-modeling studies.

Previous studies on the rat 5-HT₆ receptor have identified four residues that contribute to the ligand binding site (Boess et al., 1998): Trp102, Asp106, Ala287, and Asn290. The first three of these four residues are conserved in the mouse sequence. However, Asn290 in the rat and human TM5 is a serine (Ser290) in the mouse. Interestingly, Boess et al. (1998) mutated this residue to serine, together with an A287L mutation, and found that this increased affinity for sumatriptan and several ergopeptine ligands. We also observed an increased affinity for sumatriptan in the mouse recombinant 5-HT₆ receptor compared with rat and human (pK_i of 5.3 compared with 4.5).

From extensive site-directed mutagenesis work on other aminergic receptors, it is commonly accepted that the primary binding site for the natural agonists and most basic antagonists is the conserved aspartate on TM3 (Bikker et al., 1998; Kristiansen et al., 2000). This lies on one side of a pocket formed by residues lining the inner faces of TM4 to TM6 and "capped" on the top by residues from the second and third extracellular loops (Fig. 7). Ser290 in TM6 is one of these pocket residues. The other TM6 Ser277, which is different in the mouse and rat receptors, lies deeper in the bundle and is, in fact, oriented toward the lipid bilayer. The mutation of this to glycine might cause some change in the conformation of TM6 because of the increased flexibility, but it would not be expected to have any direct influence on ligand binding. The small, nonsignificant changes observed with certain ligands in the S277G mutant are almost certainly caused by dynamic fluctuations in the size of the cavity as a result of this greater rotational freedom around the glycine. Likewise, Ser175 is located at the top of the pocket in extracellular loop 2, and although it was predicted to be oriented into the cavity, it formed no direct interactions with

the docked ligands. Tyr188 in TM5 is the key residue, which does have significant effects on a number of the ligands studied. In the mouse receptor model, Tyr188 forms a strong hydrogen bond with Ser290, locking it in the *gauche* + rotameric state. Mutation of this serine to asparagine would normally retain the hydrogen bond. Thus, the S290N mutant has relatively little effect on ligand binding except where the asparagine has direct interactions, as in the case of Ro 04-6790 (favorable) and mianserin (unfavorable). When the *gauche* + conformation of Tyr188 in the mouse causes it to have a steric clash, as in the case of Ro 04-6790 and the rat-selective sulfonamides SB-357134 and SB-258585, then the Y188F mutation allows the aromatic ring to adopt the more favorable conformation found in the rat model. In addition to the conformational effect, the *trans* rotamer of the tyrosine causes it to have an unfavorable dipole-dipole interaction with the methoxyphenyl ring of SB-357134, and this is the cause of the lowering of binding with the rat F188Y mutant. In addition to Asp106 and the species-specific residues discussed above, all of the ligands studied are predicted to form varying interactions with a number of conserved aromatic residues in TM helices 5, 6, and 7. These observations are in accord with previous studies, for example using the 5-HT_{2A} receptor, in which conserved aromatic amino acid residues in TM5 and TM6 have been shown to be essential for agonist and antagonist binding (Roth et al., 1997; Shapiro et al., 2000). The models, as described, are thus in excellent agreement with the observed mutation results and have been used extensively in the design of further selective 5-HT₆ antagonists for this binding pocket.

In summary, we have shown that in mouse brain, the level of 5-HT₆ receptor expression is considerably lower than rat or human, and there is no enrichment in the basal ganglia. Furthermore, the mouse receptor has a distinct pharmacological profile. Using molecular biological, pharmacological, and modeling tools, we have demonstrated that two residues, Tyr188 in TM5 and Ser290 in TM6, are responsible for the observed pharmacological and structural differences between the mouse and rat/human 5-HT₆ receptors. These findings further contribute to our understanding of the structural and functional relationship between this receptor subtype and its ligands.

References

- Bentley JC, Bourson A, Boess FG, Fone KC, Marsden CA, Petit N, and Sleight AJ (1999) Investigation of stretching behaviour induced by the selective 5-HT₆ receptor antagonist, Ro 04-6790, in rats. *Br J Pharmacol* 126:1537–1542.
- Bikker JA, Trumpp-Kallmeyer S, and Humblet C (1998) G-protein coupled receptors: models, mutagenesis and drug design. *J Med Chem* 41:2911–2927.
- Blaney FE, Raveglia LF, Artico M, Cavagnera S, Dartois C, Farina C, Grugini M, Gagliardi S, Luttmann MA, Martinelli M, et al. (2001) Stepwise modulation of neurokinin-3 and neurokinin-2 receptor affinity and selectivity in quinoline tachykinin receptor antagonists. *J Med Chem* 44:1675–1689.
- Blaney FE and Tennant M (1996) Computational tools and results in the construction of G protein-coupled receptor models, in *Membrane Protein Models* (Findlay JBC ed) pp 161–176, Bios Scientific Publishers Ltd., Oxford.

- Boess FG, Monsma FJ Jr, and Sleight AJ (1998) Identification of residues in transmembrane regions III and IV that contribute to the ligand binding site of the serotonin 5-HT₆ receptor. *J Neurochem* **71**:2169–2177.
- Bourson A, Borroni E, Austin RH, Monsma FJ Jr, and Sleight AJ (1995) Determination of the role of the 5-HT₆ receptor in the rat brain: a study using antisense oligonucleotides. *J Pharmacol Exp Ther* **274**:173–180.
- Bowen WP and Jerman JC (1995) Nonlinear regression using spreadsheets. *Trends Pharmacol Sci* **16**:413–417.
- Bromidge SM, Brown AM, Clarke SE, Dodgson K, Gager T, Grassam HL, Jeffrey PM, Joiner GF, King FD, Middlemiss DN, et al. (1999) 5-Chloro-N-(4-methoxy-3-piperazin-1-yl-phenyl)-3-methyl-2-benzothiophenesulfonamide (SB-271046): a potent, selective, and orally bioavailable 5-HT₆ receptor antagonist. *J Med Chem* **42**:202–205.
- Bromidge SM, Clarke SE, Gager T, Griffith K, Jeffrey P, Jennings AJ, Joiner GF, King FD, Lovell PJ, Moss SF, et al. (2001) Phenyl benzenesulfonamides are novel and selective 5-HT₆ antagonists: identification of N-(2,5-dibromo-3-fluorophenyl)-4-methoxy-3-piperazin-1-ylbenzenesulfonamide (SB-357134). *Bioorg Med Chem Lett* **11**:55–58.
- Cheng YC and Prusoff WH (1973) Relationship between inhibition constant (K_i) and the concentration of inhibitor which causes 50% inhibition (IC₅₀) of an enzymatic reaction. *Biochem Pharmacol* **92**:881–894.
- Dunbrack RL Jr (2002) Rotamer libraries in the 21st century. *Curr Opin Struct Biol* **12**:431–440.
- East SZ, Burnet PWJ, Leslie RA, Roberts JC, and Harrison PJ (2002) 5-HT₆ receptor binding sites in schizophrenia and following antipsychotic drug administration: autoradiographic studies with [¹²⁵I]SB-258585. *Synapse* **45**:191–199.
- Funke W (1982) Proton and carbon-13 NMR spectra of mianserin and 10-hydroxymianserin derivatives in solution. Spectral assignments and conformational conclusions. *J R Neth Chem Soc* **101**:437–440.
- Gerard C, Martres MP, Lefevre K, Miquel MC, Vergé D, Lanumey L, Doucet E, Hamon M, and El Mestikawy S (1997) Immunolocalization of serotonin 5-HT₆ receptor-like material in the rat central nervous system. *Brain Res* **746**:207–219.
- Grimaldi B, Sibella-Arguelles C, Bonnin A, Fillion MP, Massot O, Rousselle JC, Seznec JC, and Fillion G (1998) Functional properties of 5-HT-moduline in the immune system: a model for central nervous system investigation. *Ann NY Acad Sci* **861**:249–250.
- Hamon M, Doucet E, Lefevre K, Miquel MC, Lanfumey L, Insausti R, Frechilla D, Del Rio J, and Verge D (1998) Antibodies and antisense oligonucleotide for probing the distribution and putative functions of central 5-HT₆ receptors. *Neuropsychopharmacology* **21**:68–76.
- Hirst WD, Abrahamsen BA, Blaney FE, Calver AR, Aloj L, Price GW, and Medhurst AD (2002) Mouse 5-HT₆ receptors: a distinct pharmacological profile from rat and human. *Soc Neurosci Abstr* **31**:641.10.
- Hirst WD, Minton JAL, Bromidge SM, Moss SF, Latter AJ, Riley G, Routledge C, Middlemiss DN, and Price GW (2000) Characterization of [¹²⁵I]-SB-258585 binding to human recombinant and native 5-HT₆ receptors in rat, pig and human brain tissue. *Br J Pharmacol* **130**:1597–1605.
- Kohen R, Fashingbauer LA, Heidmann DE, Guthrie CR, and Hamblin MW (2001) Cloning of the mouse 5-HT₆ serotonin receptor and mutagenesis studies of the third intracellular loop. *Brain Res Mol Brain Res* **90**:110–117.
- Kohen R, Metcalf MA, Khan N, Druck T, Huebner K, and Sibley DR (1996) Cloning, characterization and chromosomal localization of a human 5-HT₆ serotonin receptor. *J Neurochem* **66**:47–56.
- Kristiansen K, Kroeze WK, Willins DL, Gelber EI, Savage JE, Glennon RA, and Roth BL (2000) A highly conserved aspartic acid (Asp-155) anchors the terminal amine moiety of tryptamines and is involved in membrane targeting of the 5-HT_{2A} serotonin receptor but does not participate in activation via a “salt bridge disruption” mechanism. *J Pharmacol Exp Ther* **293**:735–746.
- Kyte J and Doolittle RF (1982) A simple method for displaying the hydropathic character of a protein. *J Mol Biol* **157**:105–132.
- Medhurst AD, Harrison DC, Read SJ, Campbell CA, Robbins MJ, and Pangalos MN (2000) The use of TaqMan RT-PCR assays for quantification of gene expression in CNS tissues and disease models. *J Neurosci Method* **98**:9–20.
- Medhurst AD, Hirst WD, Jerman JC, Meakin J, Roberts JC, Testa T, and Smart D (1999) Molecular and pharmacological characterization of a functional tachykinin NK₃ receptor cloned from the rabbit iris sphincter muscle. *Br J Pharmacol* **128**:627–636.
- Meneses A (2001) Effects of the 5-HT₆ receptor antagonist Ro 04-6790 on learning consolidation. *Behav Brain Res* **118**:107–110.
- Monsma FJ, Shen Y, Ward RP, Hamblin MW, and Sibley DR (1993) Cloning and expression of a novel serotonin receptor with high affinity for tricyclic psychotropic drugs. *Mol Pharmacol* **43**:320–327.
- Orlek BS, Borrett GT, and Smith DM (1993) Stereoselective construction of vicinal diamines. Part 1. Synthesis of fused pyrazines. *J Chem Soc* 1299–1305.
- Polczewski K, Kumasaka T, Hori T, Behnke CA, Motoshima H, Fox BA, Le Trong I, Teller DC, Okada T, Stenkamp RE, et al. (2000) Crystal structure of rhodopsin: a G protein-coupled receptor. *Science (Wash DC)* **289**:739–745.
- Roberts JC, Reavill C, East SZ, Harrison PJ, Patel S, Routledge C, and Leslie RA (2002) The distribution of 5-HT₆ receptors in rat brain: an autoradiographic binding study using the radiolabelled 5-HT₆ receptor antagonist [¹²⁵I]SB-258585. *Brain Res* **934**:49–57.
- Rogers DC and Hagan JJ (2001) 5-HT₆ receptor antagonists enhance retention of a water maze task in the rat. *Psychopharmacology (Berl)* **158**:114–119.
- Roth BL, Criago SC, Choudhary MS, Uluer A, Monsma FJ Jr, Shen Y, Meltzer HY, and Sibley DR (1994) Binding of typical and atypical antipsychotic agents to 5-hydroxytryptamine-6 and 5-hydroxytryptamine-7 receptors. *J Pharmacol Exp Ther* **268**:1403–1410.
- Roth BL, Shoham M, Choudhary MS, and Khan N (1997) Identification of conserved amino acid residues essential for agonist binding and second messenger production at 5-hydroxytryptamine_{2A} receptors. *Mol Pharmacol* **52**:259–266.
- Routledge C, Bromidge SM, Moss SF, Price GW, Hirst WD, Newman H, Riley G, Gager T, Stean T, Upton N, et al. (2000) Characterization of SB-271046: a potent, selective and orally active 5-HT₆ receptor antagonist. *Br J Pharmacol* **130**:1606–1612.
- Ruat M, Traiffort E, Arrang JM, Tardivel-Lacombe J, Diaz J, Leurs R, Schwartz JC (1993) A novel rat serotonin (5-HT₆) receptor: molecular cloning, localization and stimulation of cAMP accumulation. *Biochem Biophys Res Commun* **193**:268–276.
- Shapiro DA, Kristiansen K, Froeze WK, and Roth BL (2000) Differential modes of agonist binding to 5-hydroxytryptamine_{2A} serotonin receptors revealed by mutation and molecular modeling of conserved residues in transmembrane region 5. *Mol Pharmacol* **58**:877–886.
- Sleight AJ, Boess FG, Bos M, Levetttraft B, Riemer C, and Bourson A (1998) Characterization of Ro-04-6790 and Ro- 63–0563—potent and selective antagonists at human and rat 5-HT₆ receptors. *Br J Pharmacol* **124**:556–562.
- Stean TO, Hirst WD, Thomas DR, Price GW, Rogers D, Riley G, Bromidge SM, Serafinowska H, Smith DR, Bartlett S, et al. (2002) Pharmacological profile of SB-357134: a potent, selective, brain penetrant and orally active 5-HT₆ receptor antagonist. *Pharmacol Biochem Behav* **71**:645–654.
- Tecott LH, Chu H-M, and Brennan TJ (1998) Neurobehavioral analysis of 5-HT₆ receptor null mutant mice. The Fourth IUPHAR Satellite Meeting on Serotonin; 1998 Jul 23–25; Rotterdam, The Netherlands.
- Thompson JD, Higgins DG, and Gibson TJ (1994) CLUSTAL W: improving the sensitivity of progressive multiple sequence alignment through sequence weighting, position-specific gap penalties and weight matrix choice. *Nucleic Acids Res* **22**:4673–4680.
- Van Meerseche M and Declercq JP (1983) X-ray structure determination of mianserin. *Bull Soc Chim Belg* **92**: 307–308.
- Ward RP, Hamblin MW, Lachowicz JE, Hoffman BJ, Sibley DR, and Dorsa DM (1995) Localization of serotonin subtype 6 receptor messenger RNA in the rat brain by in situ hybridization histochemistry. *Neuroscience* **64**:1105–1111.
- Woolley ML, Bentley AJ, Sleight AJ, Marsden CA, and Fone KCF (2001) A role for 5-HT₆ receptors in retention of spatial learning in the Morris water maze. *Neuropharmacology* **41**:210–219.
- Yoshioka M, Matsumoto M, Togashi H, Mori K, and Saito H (1998) Central distribution and function of 5-HT₆ receptor subtype in the rat brain. *Life Sci* **62**:1473–1477.

Address correspondence to: Dr. Warren D. Hirst, Neurology and GI Centre of Excellence for Drug Discovery, GlaxoSmithKline, New Frontiers Science Park, Third Avenue, Harlow, Essex, CM19 5AW, United Kingdom. E-mail: Warren.D.Hirst@gsk.com
